ACS SyntheticBiology

Research Article

pubs.acs.org/synthbio

A Synthetic Biology Approach to Engineer a Functional Reversal of the β-Oxidation Cycle

James M. Clomburg,[†] Jacob E. Vick,[†] Matthew D. Blankschien,[†] María Rodríguez-Moyá,[†] and Ramon Gonzalez*[,†,‡]

[†]Department of Chemical and Biomolecular Engineering and [‡]Department of Bioengineering, Rice University, 6100 Main St., Houston, Texas 77005, United States

Supporting Information

ABSTRACT: While we have recently constructed a functional reversal of the β-oxidation cycle as a platform for the production of fuels and chemicals by engineering global regulators and eliminating native fermentative pathways, the system-level approach used makes it difficult to determine which of the many deregulated enzymes are responsible for product synthesis. This, in turn, limits efforts to fine-tune the synthesis of specific products and prevents the transfer of the engineered pathway to other organisms. In the work reported here, we overcome the aforementioned limitations by using a synthetic biology approach to construct and functionally characterize a reversal of the β-oxidation cycle. This was achieved through the *in vitro* kinetic characterization of each functional unit of the core and termination pathways, followed by their *in vivo* assembly and functional characterization. With this approach, the four functional units of the core pathway, thiolase, 3-hydroxyacyl-CoA dehydrogenase, enoyl-CoA hydratase/3-hydroxyacyl-CoA dehydratase, and acyl-CoA dehydrogenase/trans-enoyl-CoA reductase, were purified and kinetically characterized *in vitro*. When these four functional units were assembled *in vivo* in combination with thioesterases as the termination pathway, the synthesis of a variety of 4-C carboxylic acids from a one-turn functional reversal of the β-oxidation cycle was realized. The individual expression and modular construction of these well-defined core components exerted the majority of control over product formation, with only highly selective termination pathways resulting in shifts in product formation. Further control over product synthesis was demonstrated by overexpressing a long-chain thiolase that enables the operation of multiple turns of the reversal of the β-oxidation cycle and hence the synthesis of longer-chain carboxylic acids. The well-defined and self-contained nature of each functional unit makes the engineered reversal of the β-oxidation cycle "chassis neutral" and hence transferrable to the host of choice for efficient fuel or chemical production.

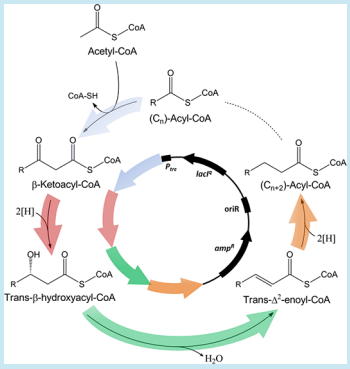

KEYWORDS: *β-oxidation reversal, Escherichia coli, biofuels and biochemicals*

The exploitation and engineering of biological systems enabling carbon-chain elongation has garnered significant attention in recent years due to the growing demand for the development of new technologies capable of producing advanced (long-chain) fuels and chemicals from renewable materials.[1−4] While the use of the fatty acid biosynthesis pathway has attracted the most attention,[5−7] a recently engineered reversal of the β-oxidation cycle shows great promise as a metabolic platform for the synthesis of alcohols and carboxylic acids of varying carbon lengths and functionalities.[8] In contrast to the fatty acid biosynthesis pathway, this pathway operates with coenzyme A (CoA) intermediates and directly uses acetyl-CoA for acyl-CoA chain elongation, characteristics that could enable product synthesis at maximum carbon and energy efficiency.[8]

Our previous work on engineering a functional reversal of the β-oxidation cycle in *Escherichia coli* focused on a top-down/system-level strategy that involved the manipulation of several global regulators.[8] A mutation that rendered FadR nonfunctional, in combination with a mutation in the cytoplasmic response regulator AtoC of the AtoSC two-component regulatory system, enabled the constitutive expression of all enzymes in the β-oxidation cycle in the absence of its natural substrate (fatty acids).[8] Since several operons encoding β-oxidation cycle enzymes are also activated by the cyclic-AMP (cAMP) receptor protein (CRP)-cAMP complex and hence repressed by the presence of alternative carbon sources, we replaced the native *crp* gene with a cAMP-independent mutant (*crp**) that confers a derepressed phenotype. Finally, since the anaerobic/microaerobic conditions used in the production of fuels and chemicals would lead to ArcA-mediated repression of most operons encoding the β-oxidation cycle, the *arcA* gene was deleted.[8] These system-level manipulations were then combined with a small set of local perturbations (elimination of native fermentation pathways and expression of selected termination pathways) to achieve the synthesis of desired products. While effective, this system-level approach has some

Special Issue: Synthetic Biology for Strain Development

Received: August 29, 2012
Published: October 16, 2012

limitations due to the ill-defined nature of the individual components of the engineered pathway. This, in turn, limits the ability to effectively manipulate such individual components to fine-tune the synthesis of specific products and prevents the transfer of the engineered pathways to other host organisms (i.e., "equivalent" global regulators would need to be engineered in other hosts to implement a functional reversal of the β-oxidation cycle).

In order to overcome the aforementioned limitations, the approach taken here focuses on a synthetic biology strategy in which the target pathway is built from well-defined and self-contained functional units that can be assembled in different combinations to achieve the synthesis of a wide array of products. This bottom-up approach implies that an effective design is created through the assembly of pre-defined components or building blocks (i.e., each functional units/enzymes composing the pathway).[9] Thus, the reconstruction of a functional reversal of the β-oxidation cycle can be accomplished without engineering global regulators and hence creating a "clean" platform that can be readily transferred to other hosts/organisms.

The implementation of the above approach entails (i) *in vitro* kinetic characterization of individual components of the pathway and (ii) *in vivo* assembly and characterization of the functional pathway. To this end, suitable enzyme(s) for each functional unit comprising the thiolase, 3-hydroxyacyl-CoA dehydrogenase, enoyl-CoA hydratase/3-hydroxyacyl-CoA dehydratase, and acyl-CoA dehydrogenase/trans-enoyl-CoA reductase elements of the core pathway (Figure 1) were purified and tested through *in vitro* kinetic characterization. We initially focused our efforts on a one-turn reversal of the β-oxidation cycle as the basic platform but selected enzymes that could also serve as a functional component of a multiple turn cycle reversal. While these four principle components encompass the entire reversal of the β-oxidation cycle, product synthesis also requires the integration of a termination pathway into the modular framework. In order to provide a functional assessment of each core unit as the pathway is built, thioesterases capable of converting each CoA pathway intermediate into their respective carboxylic acid counterpart were selected and utilized as the termination pathway(s). This approach enabled the use of carboxylic acids as proxy for product synthesis (e.g., 4-C carboxylic acids produced during a functional one-turn reversal of the β-oxidation cycle).

Once identified and characterized, the assembly and *in vivo* characterization of each functional unit of the core pathway was conducted. We selected *E. coli* as the initial chassis for pathway assembly due to its advantageous traits for industrial biofuel and biochemical production[10] and as a chassis for synthetic biology applications.[9] In addition, to demonstrate the feedstock-independent nature of the functional components (i.e., only requires the generation of acetyl-CoA from a given carbon source), glycerol was selected as the carbon source. Finally, the metabolism of *E. coli* was reprogrammed and tailored for the synthesis of 4-C and longer-chain products through local perturbations and the modular assembly of each individual component.

RESULTS AND DISCUSSION

Design of a Functional Reversal of the β-Oxidation Cycle and *in Vitro* Characterization of Its Functional Units. A functional reversal of the β-oxidation cycle results in the two-carbon elongation of an acyl-CoA intermediate per

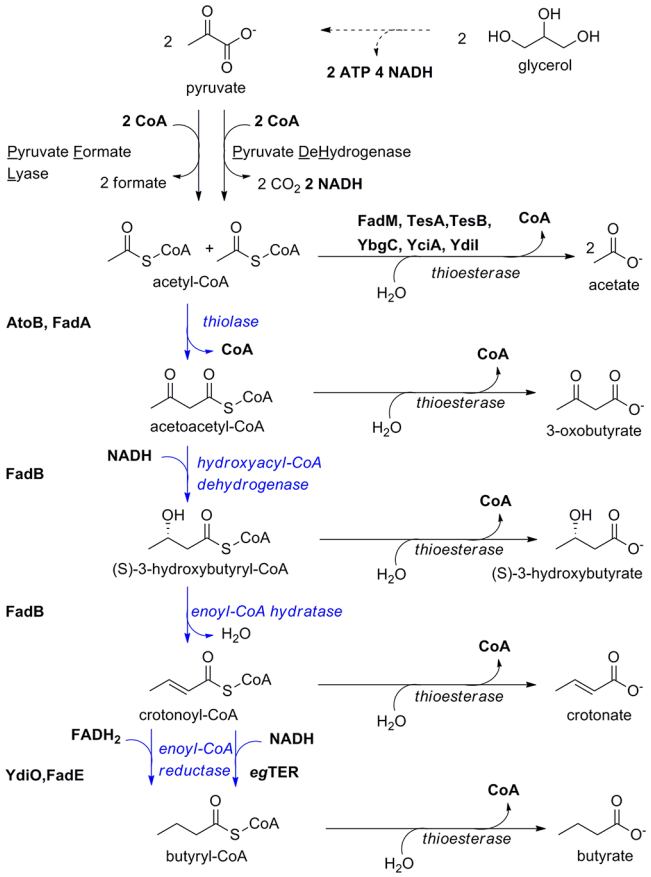

Figure 1. One-turn functional reversal of the β-oxidation cycle with 4-C carboxylic acids as a proxy for product synthesis. Core pathway enzymes represented in blue with thioesterase termination pathways resulting in carboxylic acid formation from each cycle intermediate. A multiple turn cycle involves the condensation of the end acyl-CoA molecule (butyryl-CoA from a one-turn reversal) with acetyl-CoA resulting in a 2-carbon elongation.

cycle of operation. This metabolic process requires the integration of 4 key components for core pathway function: (i) a thiolase that catalyzes the condensation of acetyl-CoA with an acyl-CoA, yielding a ketoacyl-CoA; (ii) a hydroxyacyl-CoA dehydrogenase that reduces ketoacyl-CoA to hydroyacyl-CoA; (iii) an enoyl-CoA hydratase/3-hydroxyacyl-CoA dehydratase that generates trans-enoyl-CoA from hydroxyacetyl-CoA; and (iv) an acyl-CoA dehydrogenase/trans-enoyl-CoA reductase that reduces trans-enoyl-CoA to an acyl-CoA two carbons longer than the initial acyl-CoA (Figure 1). In its simplest form, a one-turn reversal, these reactions result in the elongation of the initial acetyl-CoA molecule to butyryl-CoA. In addition to the aforementioned components, product synthesis also requires the integration of a termination pathway capable of converting each CoA pathway intermediate into the desired product. In the work reported here we used thioesterases to convert CoA thioesters intermediates into their respective carboxylic acid counterpart (Figure 1).

Thiolase. Four *E. coli* thiolases involved in the β-oxidation of fatty acids[11] (*atoB, yqeF, fadA, fadI*) can potentially catalyze the condensation of acetyl-CoA with acyl-CoA of various chain lengths. Among them, AtoB and FadA have been studied the most. AtoB exhibits higher specificity for short-chain acyl-CoA molecules,[12,13] while FadA is part of the FadBA multienzyme complex with broad chain-length specificity for acyl-CoA

dx.doi.org/10.1021/sb3000782 | ACS Synth. Biol. 2012, 1, 541−554

Table 1. *In Vitro* Kinetic Characterization of Enzymes Involved in a Functional Reversal of the β-Oxidation Cycle

enzyme	substrate[a]	k_{cat} (s^{-1})	K_M (μM)	k_{cat}/K_M (M^{-1} s^{-1})	specific activity (μmol mg^{-1} min^{-1})
AtoB	acetyl-CoA	3.17 ± 0.18	892.0 ± 56.5	(3.6 ± 0.3) × 10^3	0.919 ± 0.002[c]
	acetoacetyl-CoA	9.23 ± 0.34	68.1 ± 2.56	(1.36 ± 0.07) × 10^5	0.36 ± 0.05[c]
FadA	acetyl-CoA			7.5 ± 0.3[b]	not detected[d]
	acetoacetyl-CoA	0.75 ± 0.09	422.5 ± 57.3	(1.8 ± 0.3) × 10^3	0.013 ± 0.002[d]
FadB	acetoacetyl-CoA	25.9 ± 1.2	390.0 ± 19.2	(6.6 ± 0.4) × 10^4	0.185 ± 0.001[d]
	crotonyl-CoA			(3.2 ± 0.5) × 10^3[b]	0.051 ± 0.004[d]
*eg*TER	crotonyl-CoA	1.14 ± 0.08	98.5 ± 7.7	(1.2 ± 0.1) × 10^4	5.4 ± 0.6[e]
FadE	butyryl-CoA				0.008 ± 0.001[c]
YdiO	butyryl-CoA				0.009 ± 0.003[c]
YciA	acetyl-CoA	6.9 ± 0.1	42.7 ± 1.2	(1.62 ± 0.05) × 10^5	0.222 ± 0.007[c]
	acetoacetyl-CoA	264.6 ± 54.7	875.7 ± 180.9	(3.0 ± 0.8) × 10^5	0.672 ± 0.007[c]
	RS-3-hydroxybutyryl-CoA	32.4 ± 3.5	353.8 ± 38.8	(9 ± 1) × 10^4	0.441 ± 0.009[c]
	crotonyl-CoA	46.4 ± 7.7	1348.8 ± 235.5	(3.4 ± 0.8) × 10^4	0.27 ± 0.03[c]
	butyryl-CoA	557.5 ± 79.6	641.8 ± 91.9	(9 ± 2) × 10^5	2.9 ± 0.2[c]

[a]Direction of assay indicated by substrate and enzyme as shown in Figure 1 [b]Could not be saturated. [c]Expressed from pCA24N. [d]Expressed from pUCBB-ntH6. [e]Expressed from pTrcHis2A.

substrates.[14] Considering their well-studied nature, AtoB and FadA were selected as the most viable thiolase candidates, and further *in vitro* characterization was undertaken to ensure their compatibility in the framework of a functional β-oxidation reversal. Upon purification and kinetic characterization, AtoB was shown to effectively catalyze the condensation of two acetyl-CoA molecules with a k_{cat}/K_M of 3.6 × 10^3 M^{-1} s^{-1} showing its potential as a short-chain specific thiolase component for initiation of a one-turn β-oxidation reversal (Table 1) and hence priming a cycle of multiple turns. On the other hand, while substrate saturation with FadA during the kinetic characterization was not possible, the low estimated (see Methods) k_{cat}/K_M of 7.5 M^{-1} s^{-1} for the condensation of acetyl-CoA molecules shows FadA is not efficient for this initial condensation reaction (Table 1). It is important to note however that when one considers multiple turns of the functional reversal of the β-oxidation cycle with longer-chain-length intermediates, the broad chain-length specificity of FadA for longer-chain acyl-CoA substrates[14] could convey the ability to facilitate multiple cycle turns with a single enzyme after the initial priming of the cycle by AtoB. Also of note is the fact that both AtoB and FadA appear to be more efficient in the catabolic direction (i.e., conversion of acetoacetyl-CoA into 2 acetyl-CoA molecules), as evidenced by the significantly higher k_{cat}/K_M values for acetoacetyl-CoA compared to acetyl-CoA (Table 1). This could pose an issue during the *in vivo* assembly of components without appropriate driving forces, such as the thermodynamic driving force of metabolite pools of substrates and products,[15] in place to ensure the biosynthetic reaction is favored.

3-Hydroxyacyl-CoA Dehydrogenase. Three *E. coli* enzymes could potentially encode 3-hydroxyacyl-CoA dehydrogenase activity: two hydroxyacyl-CoA dehydrogenases (*fadB* and *fadJ*), which are involved in the β-oxidation of fatty acids,[11] and a 3-hydroxyadipyl-CoA dehydrogenase (*paaH*) that participates in the degradation of phenylacetate.[16] While involved in degradative pathways, these three enzymes catalyze reversible reactions and hence were considered viable candidates. Of the potential candidates, FadB, the second member of the FadBA multienzyme complex, is the most studied and has been shown to possess both hydroxyacyl-CoA dehydrogenase and enoyl-CoA hydratase activity with broad chain-length specificity.[17,18] Considering both of these activities are required for a functional reversal of the β-oxidation cycle and multiple cycle turns would require enzymes able to act on intermediates of varying carbon length, these key traits of FadB make it a promising candidate for *in vitro* characterization. As seen in Table 1, upon purification, FadB exhibits efficient 3-hydroxyacyl-CoA dehydrogenase activity for the NADH-dependent reduction of acetoacetyl-CoA with a k_{cat}/K_M of 6.6 × 10^4 M^{-1} s^{-1}, providing initial evidence toward its inclusion as a member of the integrated set of components.

Enoyl-CoA Hydratase. Three members of the enoyl-CoA hydratase family involved in β-oxidation reactions should be able to act as 3-hydroxybutyryl-CoA dehydratase: aerobic (*fadB*) and anaerobic (*fadJ*) enoyl-CoA hydratases that participate in the β-oxidation of fatty acids,[11] and a 2,3-dehydroadipyl-CoA hydratase (*paaF*) involved in phenylacetate degradation.[16] Despite the primary role of these enzymes in degradative pathways, the reversible nature of the reactions they catalyze indicates their potential for the dehydration of hydroxyacyl-CoAs. With the previous selection of FadB as the 3-hydroxybutyryl-CoA dehydrogenase component of a one-turn reversal of the β-oxidation cycle, this protein represents the natural choice for an enoyl-CoA hydratase (3-hydroxybutyryl-CoA dehydratase in the context of a one-turn reversal), as it is reported to encode both hydroxyacyl-CoA dehydrogenase and enoyl-CoA hydratase activities.[17,18] The selection of this enzyme would also provide the advantage of minimizing the number of required components of the integrated framework. As with 3-hydroxybutyryl-CoA dehydrogenase activity, the kinetic properties of purified FadB for 3-hydroxybutyryl-CoA dehydratase activity were evaluated (Table 1), and provided ample evidence for the ability of FadB to serve as the enoyl-CoA hydratase component in the modular framework. Although substrate saturation proved difficult, FadB did exhibit the required activity with an estimated (see Methods) k_{cat}/K_M of 3.2 × 10^3 M^{-1} s^{-1} for the hydration of crotonyl-CoA, demonstrating its potential to function as a key component during the *in vivo* assembly of a functional reversal of the β-oxidation cycle.

Acyl-CoA Dehydrogenase/trans-Enoyl-CoA Reductase. Two β-oxidation enzymes were chosen as enzymes that can potentially catalyze the last step of the reversal of the cycle: an acyl-CoA dehydrogenase (*fadE*), involved in the aerobic catabolism of fatty acids,[11] and a predicted acyl-CoA

dx.doi.org/10.1021/sb3000782 | ACS Synth. Biol. 2012, 1, 541−554

Table 2. Specific Activities of Selected Thioesterases on Relevant CoA Intermediates (μmol/mg protein/min)

enzyme[a]	acetyl-CoA	acetoacetyl-CoA	*RS*-3-hydroxybutyryl-CoA	crotonyl-CoA	butyryl-CoA	decanyl-CoA
FadM	0.0331 ± 0.0006	0.042 ± 0.004	0.009 ± 0.002	0.0017 ± 0.0003	0.027 ± 0.001	0.034 ± 0.003
TesA	0.036 ± 0.002	0.044 ± 0.005	0.02 ± 0.01	0.007 ± 0.003	0.049 ± 0.002	0.47 ± 0.04
TesB	0.030 ± 0.001	0.056 ± 0.001	0.032 ± 0.002	0.010 ± 0.001	0.101 ± 0.002	0.6 ± 0.1
YbgC	0.036 ± 0.002	0.065 ± 0.002	0.016 ± 0.004	0.006 ± 0.001	0.045 ± 0.007	0.06 ± 0.02
YciA	0.222 ± 0.007	0.672 ± 0.007	0.441 ± 0.009	0.27 ± 0.03	2.9 ± 0.2	3.7 ± 0.3
YdiI	0.036 ± 0.003	0.047 ± 0.001	0.012 ± 0.002	0.078 ± 0.005	0.0917 ± 0.0007	0.18 ± 0.04

[a]Genes encoding each protein expressed from pCA24N.

dehydrogenase (*ydiO*) proposed to be part of the β-oxidation of fatty acids under anaerobic conditions.[19] While there is evidence of YdiO[8] and FadE[20] playing roles in the reduction of crotonoyl-CoA to butyryl-CoA under certain conditions, the complexity of these enzymes make their *in vitro* characterization and *in vivo* assembly/function difficult. YdiO shares high homology with the crotonobetainyl-CoA reductase CaiA,[8] an enzyme that catalyzes the reduction of crotonobetainyl-CoA to γ-butyrobetainyl-CoA,[21] a reaction similar to the reduction of crotonyl-CoA to butyryl-CoA in the one-turn reversal of the β-oxidation cycle. Moreover, the *fixABCX* operon encoding flavoproteins and a ferredoxin required for the transfer of electrons to CaiA[22,23] shows a high sequence similarity to those encoded by the *ydiQRST* operon.[8] This suggests that, as with CaiA, YdiO requires auxiliary flavoproteins and a ferredoxin for the transfer of electrons during the reduction of enoyl-CoA to acyl-CoA making their modular assembly and *in vivo* function complicated. A further caveat for the use of these enzymes is the involvement of a ferredoxin that is oxidized during electron transfer. Reduced ferredoxin would have to be regenerated with an additional reaction to enable continued turnover of electron transfer and hence the entire functional reversal of the β-oxidation cycle. For this purpose, a predicted pyruvate:flavodoxin oxidoreductase (*ydbK*)[24] could be utilized to couple pyruvate dissimilation with ferredoxin reduction, thus enabling the continued ferredoxin-aided electron transfer to the enoyl-CoA reduction step.

While the acyl-CoA dehydrogenase FadE does not catalyze a ferredoxin-mediated reduction, the operation of this enzyme in its physiological direction (i.e., catabolism of fatty acids) is coupled to the electron transfer chain by flavoproteins and is thought to represent the only irreversible step in the catabolic operation of the β-oxidation cycle.[11] This direct coupling to the electron transfer chain with the use of FadE makes an overall one-turn functional reversal of the β-oxidation cycle unfavorable from a standard thermodynamic sense.[8] Although an electron transfer system similar to that of YdiO could be compatible with FadE, making the reaction more thermodynamically favorable, this adds a level of complexity similar to that described above for YdiO.

Given the aforementioned complexities of YdiO and FadE, we faced significant challenges during their *in vitro* purification and characterization. Upon purification, no detectable activities were measured with either enzyme, although we were able to measure their activities in crude extract of cells expressing them (Table 1). These results could reflect the requirement for auxiliary enzymes for proper function and underlie the potential challenges for their use as a key component in the modular framework. To address these issues, we used a trans-2-enoyl-CoA reductase from the photosynthetic flagellate *Euglena gracilis* (*eg*TER), shown to reduce the double bond in C4 and C6 enoyl-CoA intermediates to produce acyl-CoA via a NAD(P)H-dependent mechanism.[25] This approach eliminates the requirement for auxiliary and coupling enzymes for proper function. Interestingly, *eg*TER is a key enzyme of an anaerobic metabolic process in the mitochondrion of *E. gracilis* that leads to the synthesis of wax esters via the malonyl-CoA-independent synthesis of fatty acids (the latter a process equivalent to a functional reversal of the β-oxidation cycle).[26] This mitochondrial process synthesizes products of chain length 8−18, suggesting the ability of *eg*TER to catalyze reduction of enoyl-CoA molecules of various chain lengths.[26,27] Considering the physiological role of *eg*TER as a functional unit of a core process similar to the reversal of the β-oxidation cycle and its broad chain-length specificity, the inclusion of this enzyme in our design holds great promise. Purification and *in vitro* characterization of *eg*TER demonstrated the capability of this enzyme as the reduction of crotonyl-CoA with NADH as a cofactor proceeded with a k_{cat}/K_M of 1.2×10^4 M^{-1} s^{-1} (Table 1).

Thioesterases (Termination). The combination of the four steps described above entail the functional units that form a reversal of the β-oxidation cycle. However, product synthesis from this process requires the use of termination pathways capable of converting the CoA intermediates of the core pathway to desired products. While a wide array of products with varying functionalities can be synthesized from the cycle intermediates through the selection and integration of various termination pathways,[8] the use of thioesterases provides arguably the simplest termination pathway for the *in vivo* characterization of a functional one-turn reversal and also enables the assessment of each functional unit as the pathway is sequentially built. Thioesterases, part of the larger subfamily of hydrolase enzymes acting on ester bonds, catalyze the hydrolytic cleavage of thioester bonds. In the context of the functional reversal of the β-oxidation cycle, thioesterases cleave the thioester bond of the CoA intermediates converting them to their carboxylic acid components.

E. coli thioesterases encoded by *tesA*,[28] *tesB*,[29] *yciA*,[30] *fadM*,[31] *ydiI*,[32] and *ybgC*[32] were selected for further characterization and integration with the framework of the *in vivo* assembly due to their varying substrate specificities. *In vitro* characterization through specific activity measurements of crude cell extract of strains expressing these various thioesterases showed YciA has the highest activity on 4-C CoA intermediates of the cycle (Table 2). However, each of the tested thioesterases showed increased activity with the longer-chain intermediate decanoyl-CoA (Table 2). While the high activity of YciA for the relevant 4-carbon CoA intermediates is promising, one possible issue revealed in this characterization is the fact that YciA also appears to have significant activity toward acetyl-CoA (Table 2), which could result in competition between the cycle initiation (thiolase) and the termination pathway in this case. This was confirmed through a full kinetic characterization of

YciA, as the K_M for acetyl-CoA (42.7 μM) was significantly lower than the K_M for acetyl-CoA of AtoB (892 μM) (Table 1). In addition, this analysis revealed that YciA exhibits significant catalytic efficiency for all potential CoA intermediates during a one-turn reversal of the β-oxidation cycle (Table 1), suggesting its ability to serve as the termination pathway from any CoA intermediate during the integrated assembly of the modules. However, given the low K_M and high catalytic efficiency of YciA for acetyl-CoA, overexpression of this enzyme could also limit the flux into the core pathway during the *in vivo* assembly of a functional reversal of the β-oxidation cycle, and thus the testing of all selected thioesterase components is required to determine optimal functionality.

***In Vivo* Assembly of Functional Units Required for a One-Turn Reversal of the β-Oxidation Cycle: 4-C Carboxylic Acids As Proxy for Product Synthesis.** While the *in vitro* characterization of selected components provides evidence of the ability of these enzymes to perform the reactions required for a functional reversal of the β-oxidation cycle, only the *in vivo* assembly of these individual units in conjunction with selected thioesterases as termination pathways can provide an assessment of pathway functionality (i.e., synthesis of 4-C carboxylic acids) (Figure 1). This type of synthetic/bottom-up approach also ensures that each predefined component or building block (i.e., each functional unit/enzyme composing the pathway) can be individually integrated enabling a true assessment of the role and functionality of each step in a one-turn reversal of the core pathway.

However, before this can be achieved, the metabolism of the host organism (e.g., *E. coli* for our purposes) must be reprogrammed to ensure that the expression of the individual components of the core and termination pathways leads to the desired biochemical product(s). Considering glycerol as the carbon source of interest, this requires shifting *E. coli* metabolism away from native fermentation products (Figure 2a) and ensuring the generation of acetyl-CoA to serve as the priming molecule of the core pathway (Figure 1). To this end, a strain containing deletions of genes encoding enzymes responsible for fermentative routes to ethanol (*adhE*), acetate (*pta* and *poxB*), lactate (*ldhA*), and succinate (*frdA*) was constructed. As a result of these key gene deletions, glycerol metabolism was shifted from a mixture of lactate, acetate, and ethanol to a mixture of pyruvate and acetate in the engineered host (MG1655 Δ*ldhA*Δ*poxB*Δ*pta*Δ*adhE*Δ*frdA*, JC01) (Figure 2a). This product profile indicates that metabolism within the engineered host/chassis is adequately tailored for the synthesis of the desired 4-C carboxylic acids from the core pathway, as both the production of pyruvate and acetate reflect the build-up of the acetyl-CoA pool (Figure 1). As such, the expression of a thiolase with high specificity for short-chain acyl-CoA compounds (i.e., AtoB) within this host should provide an additional outlet for acetyl-CoA, serving as the initial priming step of the core pathway and enabling the *in vivo* assessment of the individual components required for a functional reversal of the β-oxidation cycle.

As expected, the individual overexpression of *atoB* in JC01 resulted in the production of 4-C carboxylic acids (Figure 2a), demonstrating that AtoB can serve to initiate the cycle under these conditions as well as indicating that natively expressed thioesterase(s) are present to serve as the termination pathway for the initial *in vivo* assessment of the cycle. However, somewhat unexpected was the distribution of 4-C carboxylic acid products resulting from *atoB* expression. 3-Oxobutyrate,

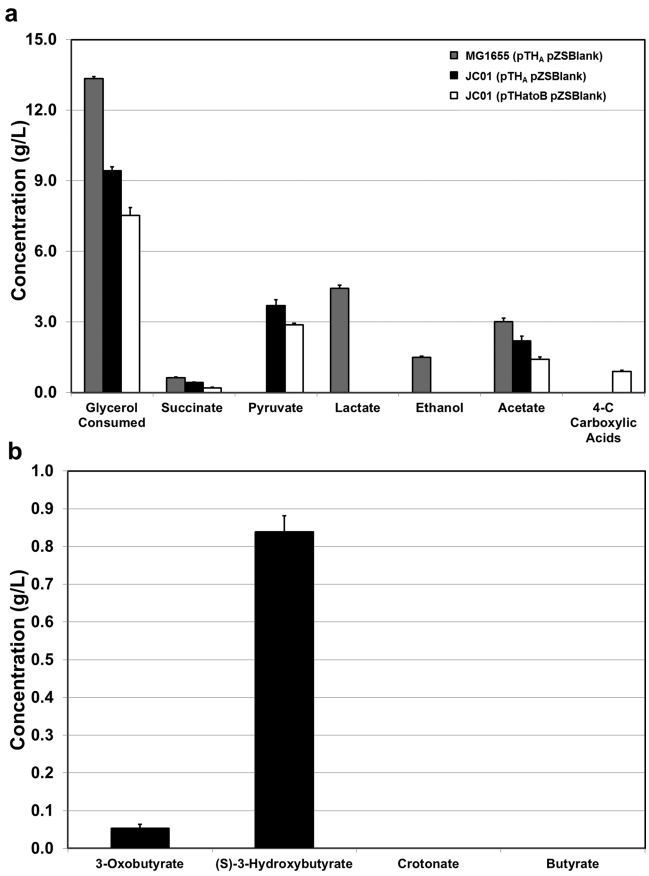

Figure 2. Reprogramming host metabolism for the *in vivo* assembly of the individual components of a β-oxidation reversal. (a) Glycerol consumption and product synthesis in wild-type *E. coli* MG1655 and engineered strain JC01 (MG1655 Δ*ldhA*Δ*poxB*Δ*pta*Δ*adhE*Δ*frdA*) with control vectors pTH$_A$ and pZSBlank, and JC01 with thiolase (AtoB) overexpression. (b) Distribution of 4-C carboxylic acids produced upon thiolase overexpression in JC01, i.e., JC01 (pTHatoB pZSBlank). Gene overexpression apparent from plasmid names (i.e., pTHatoB expressing *atoB*).

the carboxylic acid product of thiol cleavage of acetoacetyl-CoA, was present only in small amounts, while the majority of the 4-C carboxylic acid production was in the form of 3-hydroxybutyrate, the thioesterase cleavage product of 3-hydroxybutyryl-CoA (Figure 2b). This result probably indicates that the natively expressed thioesterase(s) under these conditions could have a very low specificity for acetoacetyl-CoA, and/or the accumulation of acetoacetyl-CoA prompts its reduction to 3-hydroxybutyryl-CoA through the action of a native 3-ketobutyryl-CoA dehydrogenase (Figure 1). In order to investigate these possibilities and provide further assessment of selected termination pathway enzymes, strains were constructed in which *atoB* overexpression was combined with either overexpression of a thioesterase (*tesA*, *tesB*, *yciA*, *fadM*, *ydiI*, *ybgC*) or their deletion from the chromosome of the host strain. While no clear indication of a key thioesterase for 3-oxobutyrate production was determined, as no single overexpression significantly increased or single deletion unambiguously abolished 3-oxobutyrate (Figure 3), several notable aspects are seen. First, while the expression of *ybgC* does not yield an increase in 3-oxobutyrate, acetone production is observed in this strain (Figure 3a). Acetone, a highly volatile short-chain methyl ketone, can be formed from the

dx.doi.org/10.1021/sb3000782 | *ACS Synth. Biol.* 2012, 1, 541−554

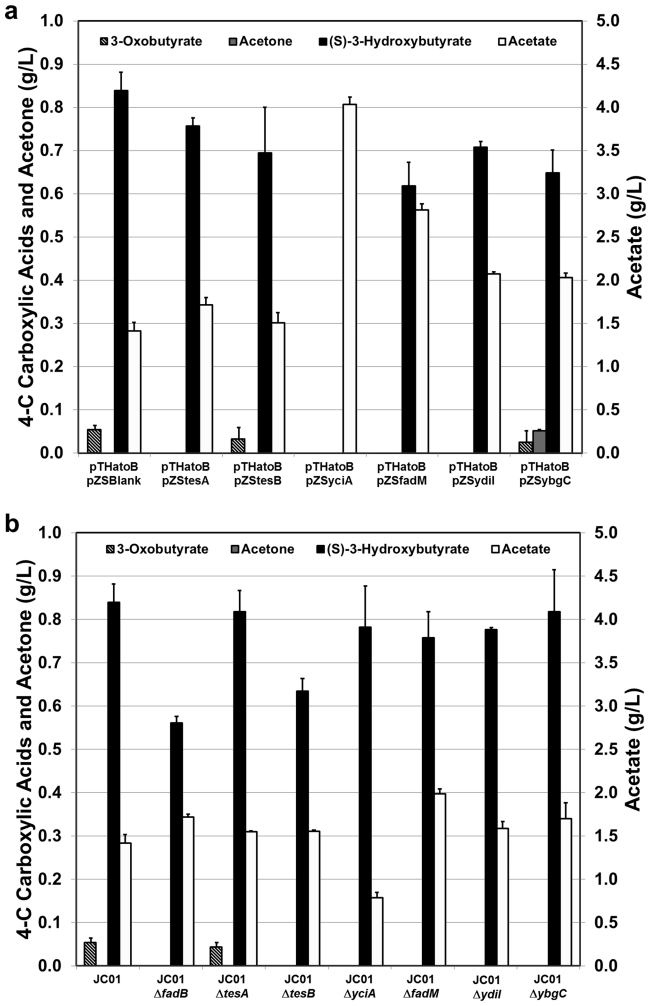

Figure 3. Impact of thiolase overexpression and termination pathway manipulation. (a) 4-C carboxylic acid and acetone production in JC01 upon thiolase (AtoB) overexpression in combination with thioesterase overexpression. (b) 4-C carboxylic acid and acetone production in JC01 harboring pTHatoB and pZSBlank with native 3-hydroxyacyl-CoA dehydrogenase (FadB) or thioesterase chromosomal deletion. Gene overexpression apparent from plasmid names (i.e., pZStesA expressing *tesA*). Δ"*gene*" represents gene deletion.

spontaneous decarboxylation of 3-oxobutyrate under appropriate conditions.[33] Second, and perhaps most notable, is the fact that overexpression of *yciA* leads to the elimination of all 4-C carboxylic acid products of the core pathway and resulted in a nearly 3-fold increase in the production of acetate (Figure 3a). While the results of the *in vitro* analysis of YciA indicated that this thioesterase can act on the majority of pathway intermediates seen from a one-turn reversal of the *β*-oxidation cycle (Table 1), the large increase in acetate reinforces the conclusion from *in vitro* characterization that the lower K_M and greater catalytic efficiency (Table 1) allows YciA to favorably compete with AtoB for acetyl-CoA when overexpressed at significant levels. In addition, the reversible nature of AtoB (Table 1) and lack of an individually expressed 3-ketobutyryl-CoA dehydrogenase to act on acetoacetyl-CoA (Figure 1) could also underlie the increased acetate production upon *yciA* overexpression. This also indicates that the overall control of product formation in the case of the expression of individual components may lie within the core pathway as opposed to the termination pathway.

The latter scenario is reflected by the fact that significant amounts of 3-hydrobutyrate are observed upon *atoB* expression (Figure 2b), even in the lack of independent expression of a 3-ketobutyryl-CoA dehydrogenase. This result also provides a means of further assessing native FadB function as 3-ketobutyryl-CoA dehydrogenase during a reversal of the *β*-oxidation cycle. For this purpose, the *fadB* gene was deleted from the host strain, and 4-C carboxylic acid production was tested upon overexpression of *atoB* (i.e., JC01 Δ*fadB* pTHatoB pZSBlank). As seen in Figure 3b, the deletion of *fadB* led to a ∼1.5-fold decrease in 3-hydrobutyrate production when compared to JC01 pTHatoB pZSBlank, reflecting a significant role of natively expressed *fadB* in the conversion of acetoacetyl-CoA to 3-hydrobutyryl-CoA. However, the deletion of *fadB* did not completely abolish 3-hydrobutyrate production, indicating that other enzymes could be playing a role in this conversion. As previously mentioned, possible candidates include an anaerobic hydroxyacyl-CoA dehydrogenase (*fadJ*) and a 3-hydroxyadipyl-CoA dehydrogenase (*paaH*), with the latter showing moderate specific activity toward the reduction of acetoacetyl-CoA when the purified enzyme was tested (data not shown). While these results provide an intriguing area for further assessment of enzymes capable of catalyzing this reaction, both the *in vitro* characterization and the role of FadB upon *atoB* overexpression reflect the potential for this enzyme to serve as a key functional unit of the reversal of the *β*-oxidation cycle.

In order to further assess FadB and integrate the 3-hydroxyacyl-CoA dehydrogenase and enoyl-CoA hydratase components into the modular framework, a controllable construct for both *atoB* and *fadB* expression (i.e., pTHatoB.-fadB) was assembled and tested *in vivo* for 4-C carboxylic acid production. Further demonstrating the ability for this enzyme to serve as a key component of the reversal of the *β*-oxidation cycle, the combined overexpression of *atoB* and *fadB* in JC01 lead to a 3-fold increase in 3-hydroxybutyrate production compared to *atoB* expression only, with 2.5 g/L of 3-hydroxybutyrate produced at a yield of 0.29 g/g (Figure 4). Interestingly, despite the fact the *in vitro* characterization of FadB (Table 1) indicates that this enzyme can serve as both a 3-ketobutyryl-CoA dehydrogenase and 3-hydroxybutyryl-CoA dehydratase during the reversal of the *β*-oxidation cycle, only increases to 3-hydroxybutyrate production were observed upon its expression with *atoB*, with no detectable crotonate, the thiol cleavage product of crotonoyl-CoA (Figure 1) observed. This is likely a result of the specificity of the native thioesterase(s) active under these conditions rather than a reflection of the *in vivo* ability for FadB to perform the dehydration reaction, as small amounts of butyrate, requiring the reduction and subsequent thioesterase cleavage of crotonoyl-CoA (Figure 1), are also seen with this strain (Figure 4a). This was further assessed through the combined expression of *atoB* and *fadB* with either selected thioesterase individual overexpression (Figure 4a) or deletion (Figure 4b). While no increases to 3-hydroxybutyrate were observed upon the overexpression of selected thioesterases, the overexpression of *ydiI* in conjunction with *atoB* and *fadB* resulted in the production of small amounts of crotonate (∼0.2 g/L, Figure 4a), suggesting the ability for this enzyme to serve as a termination pathway for crotonate production and further confirming the ability for FadB to catalyze both the first reduction and subsequent dehydration reactions of the cycle. Also of note is the fact that despite the high specific activities and catalytic efficiency of YciA for 3-

dx.doi.org/10.1021/sb3000782 | *ACS Synth. Biol.* 2012, 1, 541–554

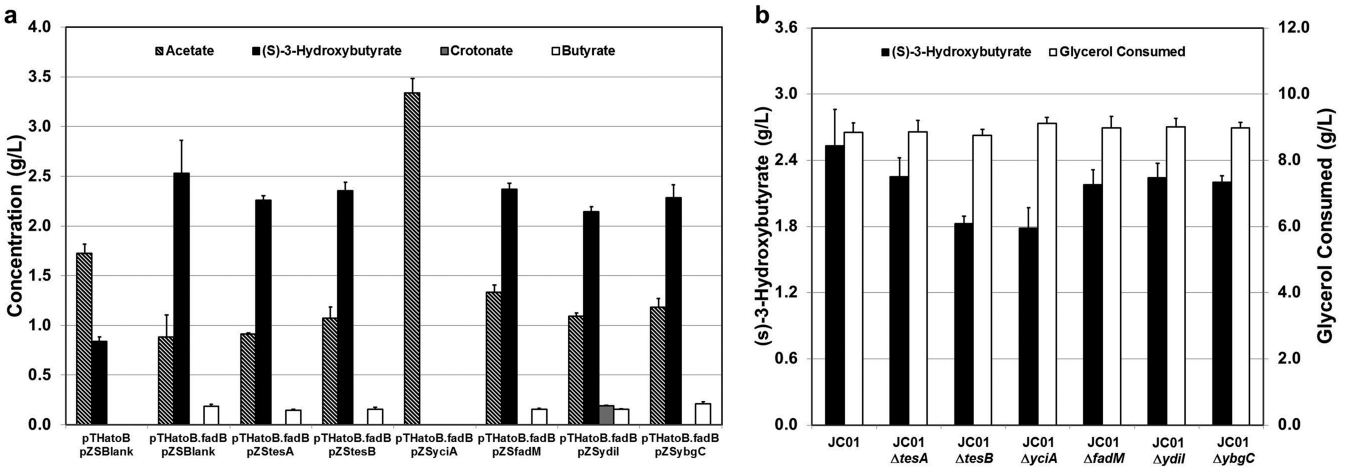

Figure 4. *In vivo* assembly of the thiolase, 3-hydroxyacyl-CoA dehydrogenase, and enoyl-CoA hydratase components of a one-turn β-oxidation reversal. (a) 4-C carboxylic acid and acetate production in JC01 with AtoB and FadB expression in conjunction with thioesterase overexpression. (b) Impact of native thioesterase chromosomal deletion on (*S*)-3-Hydroxybutyrate production and glycerol consumption in the host strain harboring pTHatoB.fadB and pZSBlank. Gene overexpression apparent from plasmid names (i.e., pZStesA expressing *tesA*). Δ"*gene*" represents gene deletion.

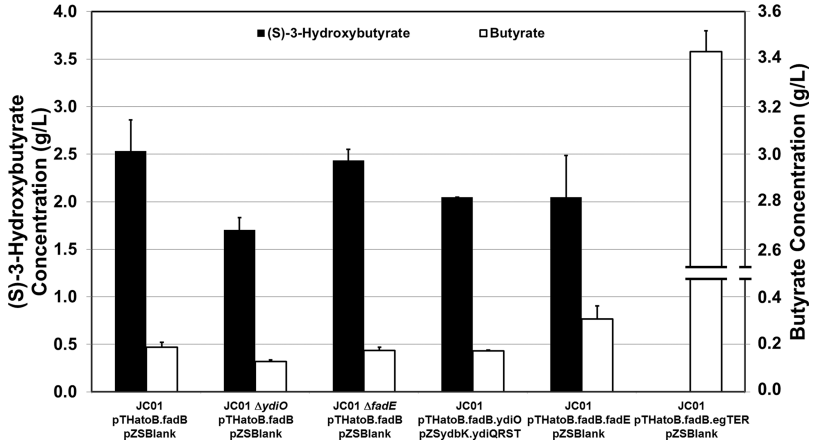

Figure 5. Functional assessment of candidate acyl-CoA dehydrogenase/trans-enoyl-CoA reductase enzymes during the *in vivo* assembly of a full one-turn β-oxidation reversal. (*S*)-3-Hydroxybutyrate and butyrate production with AtoB and FadB overexpression in the host strain combined with native acyl-CoA dehydrogenase (*fadE*, *ydiO*) chromosomal deletion or acyl-CoA dehydrogenase/trans-enoyl-CoA reductase (*eg*TER) expression. Gene overexpression apparent from plasmid names (i.e., pTHatoB.fadB.egTER expressing *atoB*, *fadB*, and *eg*TER). Δ"*gene*" represents gene deletion.

hydroxybutyryl-CoA and crotonoyl-CoA (Table 1), the combined overexpression of *yciA* with *atoB* and *fadB* results in increased acetate production with complete elimination of 4-C carboxylic acid pathway products (Figure 4a), mirroring the results upon *yciA* overexpression with *atoB* only (Figure 3a). These results again underlie the importance of placing the main level of control over product formation on the individual steps expressed from the core pathway and supplementing this structure with highly specific termination pathways leading to specific product formation (such as the case of *ydiI* expression and crotonate formation). The promiscuity of the selected thioesterases, specifically YciA, for multiple pathway intermediates (Table 1) as well as the competition for intermediates between enzymes within the core pathway and termination pathways creates an intricate balance between the expression levels of key enzymes. For the purposes of 4-C carboxylic acid production, it appears to be better to utilize native host termination pathway(s) as a means of complementing the manipulation of the individual functional units of the core pathway as the overall control strategy for the synthesis of different products. For the case of 3-hydroxybutyrate formation in *E. coli*, select thioesterase deletion in conjunction with *atoB* and *fadB* expression indicate that while native expression of *tesB* and *yciA* may play a role in its production, as evidenced by the slight decreases in production levels (Figure 4b), no single native termination pathway from the selected thioesterases is solely responsible for 3-hydroxybutyrate production.

Further evidence to the control over product formation that the core pathway exerts is seen from the presence of butyrate when *atoB* and *fadB* are individually expressed (even in conjunction with selected thioesterases other than the aforementioned *yciA*, Figure 4a). Similar to the production of 3-hydroxybutyrate with thiolase expression only, the production of butyrate upon the expression of *atoB* and *fadB* would require the native expression of enzymes capable of catalyzing core pathway reactions, specifically the presence of a butyryl-CoA dehydrogenase required for the reduction of crotonyl-CoA to butyryl-CoA (Figure 1). In an attempt to elucidate the native enzymes involved in this conversion, gene deletions of candidates, including an acyl-CoA dehydrogenase (*fadE*) and a predicted acyl-CoA dehydrogenase (*ydiO*), were singularly added to JC01 and tested in combination with the expression of

dx.doi.org/10.1021/sb3000782 | *ACS Synth. Biol.* 2012, 1, 541–554

atoB and *fadB* (Figure 5). While no single deletion resulted in the complete elimination of butyrate production, the deletion of *ydiO* resulted in a ~30% decrease in butyrate concentration, indicating a possible role for this predicted acyl-CoA dehydrogenase (Figure 5). To gain further insight to the possible role and ability of these enzymes to serve as a key component of a functional reversal of the β-oxidation cycle, constructs that enable the combined overexpression of *fadE* or *ydiO* in conjunction with the thiolase (AtoB), 3-hydroxyacyl-CoA dehydrogenase (FadB), and enoyl-CoA hydratase components (FadB) were developed (i.e., pTHatoB.fadB.fadE and pTHatoB.fadB.ydiO). It is also important to note that for the case of *ydiO* expression, a vector containing the predicted auxiliary enzymes required for proper enzyme/pathway function (see previous section) was also constructed (i.e., pZSydbK.ydiQRST) and tested with the aforementioned construct in the presence of 1 mM thiamine pyrophosphate (TPP), shown to increase YdbK activity.[24] As seen in Figure 5, while the expression of *ydiO*, even with the coexpression of auxiliary enzymes, showed no increase in butyrate production over *atoB* and *fadB* expression only, the expression of *fadE* with the first two enzymes of the core pathway resulted in a ~60% increase in butyrate levels, showing the ability of this enzyme to contribute during the reversal of the β-oxidation cycle. While these results indicate a role for YdiO and FadE, the low levels of butyrate and high levels of 3-hydroxybutryate production by these strains reflect the complexities involved with the use of these enzyme systems (e.g., requirement for additional auxiliary enzymes and coupling partners such as YdbK and YdiQRST) (see previous sections).

As previously discussed, an alternative component for this step is the use of the trans-2-enoyl-CoA reductase from *E. gracilis* (*eg*TER), which not only shows favorable kinetic characteristics for the reduction of crotonyl-CoA (Table 1) but is also from an organism that has been shown to possess a metabolic process (synthesis of waxes) whose core pathway is essentially equivalent to a functional reversal of the β-oxidation cycle.[26] *eg*TER does not require auxiliary enzymes or coupling reactions for proper function as NAD(P)H is used as the electron donor in the reaction.[25] While the lack of a requirement for auxiliary enzymes could help the efficiency of this enzyme when used with a variety of carbon sources, in the case of glycerol, the fact that NADH is used as the reducing equivalent also confers an advantage for the production of reduced compounds that can be achieved from the intermediates of the cycle. The reduced nature of glycerol dictates that the formation of one molecule of pyruvate generates twice the number of reducing equivalents (2 NADH) as that from glucose,[34] representing the exact number of reducing equivalents required for each "turn" of the cycle (i.e., two reduction reactions from the ketoacyl-CoA to the acyl-CoA intermediate, Figure 1). In contrast to the use of YdiO, which requires the regeneration of a reduced ferredoxin during pyruvate dissimilation due to the nature of the electron donor for these enzymes, the fact that *eg*TER utilizes NADH results in the ability to use this enzyme in conjunction with pyruvate dissimilation through pyruvate formate lyase to avoid the accumulation of additional reducing equivalents.

Given these distinct advantages of *eg*TER compared to other candidate butyryl-CoA dehydrogenases, we investigated the impact of the combined expression of *atoB*, *fadB*, and *eg*TER, encoding all components required in the modular framework for an efficient one-turn reversal of the β-oxidation cycle. As seen in Figure 5, in stark contrast to the expression of either *fadE* or *ydiO*, the expression of *eg*TER along with *atoB* and *fadB* resulted in significant butyrate levels (3.43 g/L at a yield of 0.35 g/g produced). In addition, no 3-hydroxybutyrate was produced by this strain (Figure 5), showing both the efficiency of *eg*TER for this reduction reaction, as well as further demonstrating the ability of the core pathway components to dictate product formation during a one-turn reversal of the β-oxidation cycle. Additional confirmation to this second point was provided through the expression of the key components required for a full one-turn reversal in conjunction with individual thioesterase overexpression in the host strain. No significant increase in butyrate production was observed upon overexpression of any of the thioesterases (Figure 6a), despite moderate specific activities for butyryl-CoA (Table 2). However, while *yciA* expression led to significant increases in acetate production, its expression did not completely eliminate 4-C carboxylic acid production as it had with *atoB* or *atoB*/*fadB* expression only (Figure 6a). This likely reflects the strong

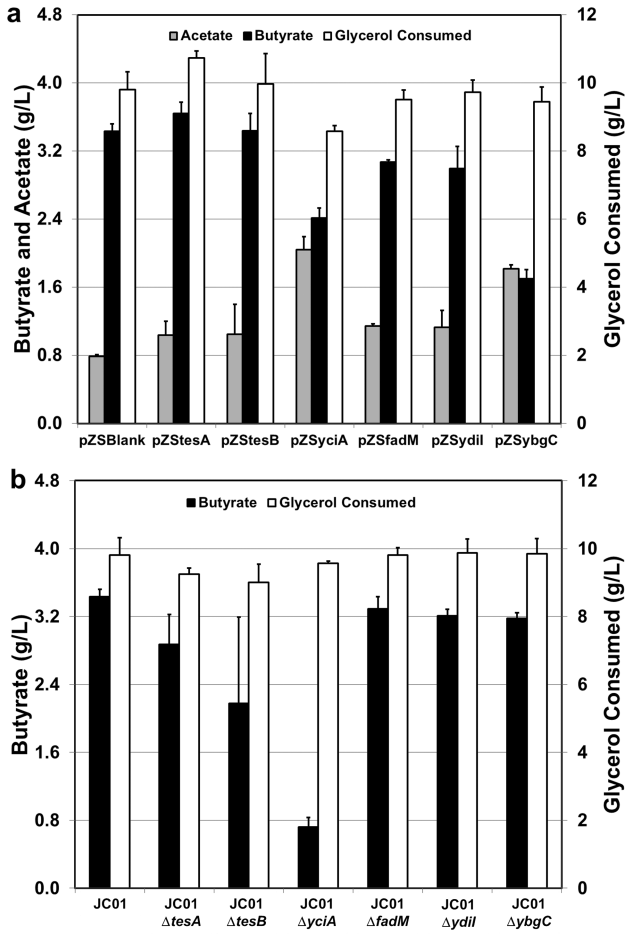

Figure 6. Termination pathway manipulation with a functional full one-turn β-oxidation reversal. (a) Glycerol consumption, butyrate, and acetate production in JC01 upon thiolase (AtoB), 3-hydroxyacyl-CoA dehydrogenase (FadB), enoyl-CoA hydratase (FadB), and trans-enoyl-CoA reductase (*eg*TER) expression (i.e., pTHatoB.fadB.egTER) in combination with thioesterase overexpression via controllable construct. (b) Glycerol consumption and butyrate production in JC01 harboring pTHatoB.fadB.egTER and pZSBlank with native thioesterase chromosomal deletion. Gene overexpression apparent from plasmid names (i.e., pTHatoB.fadB.egTER expressing *atoB*, *fadB*, and *eg*TER). Δ"*gene*" represents gene deletion.

dx.doi.org/10.1021/sb3000782 | *ACS Synth. Biol.* 2012, 1, 541–554

driving force to butyryl-CoA synthesis the expression of *eg*TER dictates (i.e., core pathway expression controlling overall product formation), in combination with the high catalytic efficiency and specific activity for butyryl-CoA that YciA shows compared to other 4-C CoA intermediates (Table 1), thus minimizing the impact of YciA activity on acetyl-CoA. Also of note is the fact that the *ybgC* expression, which had not previously shown an impact on 4-C carboxylic acid production, resulted in a significant decrease in butyrate concentration in this instance.

While the modular expression of the individual components of a functional reversal of the β-oxidation cycle appears to exert the most control over the products produced with thioesterase termination pathways, the subsequent deletion of native thioesterases in JC01 with *atoB*, *fadB*, and *eg*TER expression does provide valuable insight into the identity of the native termination pathway to butyrate. Despite the ambiguous nature of thioesterase deletion with partial β-oxidation cycle component expression, for a full one-turn cycle reversal YciA appears to be the most critical thioesterase for butyrate production as the deletion of *yciA* resulted in a near 5-fold decrease in butyrate concentration and yield (Figure 6b). These results agree with the high catalytic efficiency observed for YciA when butyryl-CoA is used as a substrate compared to other 4-C CoA intermediates (Table 1) and the fact that no other thioesterase tested has near the levels of specific activity on butyryl-CoA as YciA (Table 2). Despite the fact that YciA appears critical for butyrate production and also exhibits high activity for all pathway intermediates of a one-turn reversal (Table 1), its overexpression actually resulted in a decrease in 4-C carboxylic acid product formation when combined with the expression of individual core pathway enzymes due to the promiscuous nature of this thioesterase for a broad range of substrates.[30]

Overall, the *in vivo* assembly of the individual components of the cycle with 4-C carboxylic acids as the proxy for product synthesis demonstrated what functional units are required for the effective functioning of the pathway. This enabled the construction of a fully synthetic and transferable system for the core components of a one-turn reversal the β-oxidation cycle. With this in place, the determination of the key requirements and components needed to extend the core pathway for multiple turns can be assessed, thus expanding the scope of products that can be synthesized through a functional reversal of the β-oxidation cycle.

Synthesis of Longer-Chain Products by Operating Multiple Turns of a Functional Reversal of the β-Oxidation Cycle. The operation of multiple turns of a reversal of the β-oxidation cycle requires the condensation of the acyl-CoA generated from a turn(s) of the cycle with an additional acetyl-CoA molecule to lengthen the acyl-CoA by 2 carbons each cycle turn (e.g., condensation of butyryl-CoA with acetyl-CoA in Figure 1).[8] Thus, the initiation and extension of multiple cycle turns requires the use of a thiolase(s) with specificity for longer-chain acyl-CoA molecules combined with other core pathway enzymes capable of acting on intermediates of increasing carbon number. While the selection and functionality of *E. coli* FadB and *eg*TER from *E. gracilis* for a one-turn reversal of the β-oxidation cycle demonstrated the reversible nature and capability of these enzymes, another advantage of their selection is the fact that they have been shown to participate in metabolic processes involving intermediates of various chain lengths and hence should have the ability to act on a broad range of carbon length intermediates (see previous sections). Therefore, with the current module enabling a functional reversal of the β-oxidation cycle, the key step controlling the ability to operate multiple turns of cycle lies with the thiolase selected for the condensation of acyl-CoA intermediates. While AtoB was chosen for a one-turn reversal due to its higher specificity for short-chain acyl-CoA molecules,[12,13] this trait may limit its ability to operate for continued turns of the cycle involving increasing carbon length intermediates. On the other hand, FadA exhibits broad chain-length specificity for acyl-CoA substrates,[14] making this enzyme an ideal candidate to support multiple cycle turns and enabling the production of longer-chain products. However, the low efficiency of FadA with acetyl-CoA as a substrate (Table 1) likely requires the presence of another thiolase with higher specificity for short-chain acyl-CoA molecules (such as AtoB) to perform the initial condensation reaction (i.e., priming of the cycle). Utilizing these components, a platform for the operation of multiple turns of a functional reversal of the β-oxidation cycle was developed through the modular construction of vectors encoding AtoB, the FadBA operon, and *eg*TER. When integrated in the host strain JC01, this design enabled synthesis of extracellular longer-chain fatty acids up to C12 (dodecanoic acid) through the native expression of thioesterase termination pathways (Figure 7). The expression of *fadA* was critical for this

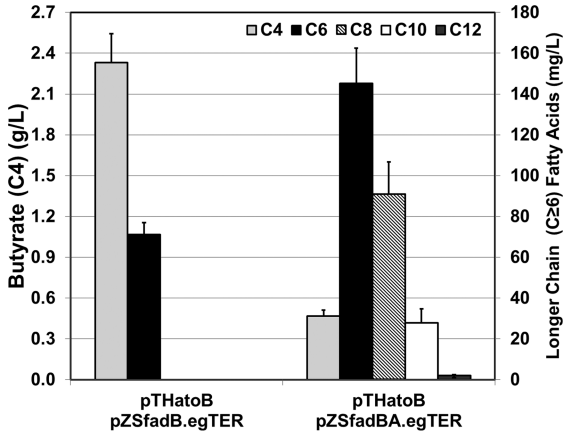

Figure 7. Operation of multiple cycle turns during a functional reversal of the β-oxidation cycle for the synthesis of longer-chain products. Distribution of extracellular fatty acid production by JC01 upon the expression of the functional units for a full one-turn reversal (pTHatoB pZSfadB.egTER) and with the inclusion of the long-chain specific thiolase FadA (pTHatoB pZSfadBA.egTER). C6, hexanoic (caproic) acid; C8, octanoic (caprylic) acid; C10, decanoic (capric) acid; C12, dodecanoic (lauric) acid. Gene overexpression apparent from plasmid names (i.e., pZSfadBA.egTER expressing *fadB*, *fadA*, and *eg*TER).

purpose, as the same integrated components produced significantly less total longer-chain fatty acids (C ≥ 6) in the absence of FadA, and no products greater than C6 were detected (Figure 7). In addition, 5 times the amount of butyrate was observed when FadA was excluded as a modular component, indicating the difficulty for AtoB to efficiently operate multiple cycle turns (and the ability of FadA to outcompete termination at butyrate). While this modular framework demonstrates the required components for the operation of multiple cycle turns during a functional reversal of the β-oxidation cycle, the relatively low levels of longer-chain

dx.doi.org/10.1021/sb3000782 | *ACS Synth. Biol.* 2012, 1, 541–554

fatty acids demonstrate the opportunity for future investigation into the overall integration of the core pathway components as well as the identification and incorporation of highly specific termination pathways enabling the production of a wide array of products with varying carbon length and functionality.

Conclusions. An engineered reversal of the β-oxidation cycle was constructed using a synthetic/bottom-up approach based on the *in vitro* kinetic characterization of individual functional units and their *in vivo* assembly. This strategy enabled the synthesis of a variety of 4-C carboxylic acids resulting from a one-turn functional reversal of the β-oxidation cycle, as the individual thiolase (AtoB), 3-hydroxyacyl-CoA dehydrogenase (FadB), enoyl-CoA hydratase (FadB), and acyl-CoA dehydrogenase/trans-enoyl-CoA reductase (*eg*TER) components exerted the majority of the control over product formation with native thioesterase termination pathways. Through the integration of a thiolase capable of acting on longer-chain intermediates (FadA), the initiation of multiple cycle turns leading to the production of longer-chain products was also demonstrated. This modular framework for the synthesis of 4-C and higher compounds overcomes some limitations with the previously used system-level/top-down approach (due to the ill-defined nature of the individual components of the pathway), providing a "clean" platform that can be transferred to other hosts/organisms. The self-contained and host-independent functional units identified in this study provide the core metabolic platform required for the efficient production of a wide array of compounds attainable from key intermediates of the reversal of the β-oxidation cycle. Further identification and integration of selective termination pathways should provide the required functionality to expand the portfolio of components. This combined with further optimization should enable the integration of this pathway within other industrial hosts allowing the advantageous nature of a reversal of the β-oxidation cycle to be fully exploited for the synthesis of a wide array of drop-in biofuels and biochemicals.

METHODS

Strains, Plasmids, and Genetic Methods. Wild-type K12 *Escherichia coli* strain MG1655[35] was used as the host for all genetic modifications. Gene knockouts were introduced in MG1655 and its derivatives by P1 phage transduction.[36,37] Single gene knockout mutants from the National BioResource Project (NIG, Japan)[38] were used as donors of specific mutations. All mutations were confirmed by polymerase chain reaction, and the disruption of multiple genes in a common host was achieved as previously described.[36] All resulting strains used in this study are listed in Supplementary Table S1.

Gene overexpression was achieved by cloning the desired gene(s) in either low-copy (pZS[36]) or higher copy based vectors (pTrcHis2A, abbreviated pTH_A; Invitrogen, Carlsbad, CA) utilizing In-Fusion PCR cloning technology (Clontech Laboratories, Inc., Mountain View, CA). Cloning inserts were created via PCR of ORFs of interest from *E. coli* genomic DNA using the primers listed in Supplementary Table S2 with Phusion DNA polymerase under standard conditions described by the supplier (Thermo Scientific, Waltham, MA). Amplification of the trans-2-enoyl-CoA reductase gene from *E. gracilis* (*eg*TER) was performed as above except using a plasmid harboring a codon-optimized *eg*TER synthesized by GenScript (Piscataway, NJ). When appropriate, a RBS was added via primer synthesis. Vector backbone was purified from *E. coli* cultures (Qiagen, Valencia, CA) and digested with the restriction enzymes listed in Supplementary Table S2 as according to the manufacturer (New England Biolabs, Ipswich, MA) to enable cloning. The resulting In-Fusion products were used to transform *E. coli* Stellar cells (Clontech Laboratories, Inc., Mountain View, CA), and positive clones were confirmed by PCR, restriction digestion, and DNA sequencing.

All molecular biology techniques were performed with standard methods[37,39] or by manufacturer protocol. Strains were kept in 32.5% glycerol stocks at −80 °C. Plates were prepared using LB medium containing 1.5% agar, and appropriate antibiotics were included at the following concentrations: ampicillin (100 μg/mL), kanamycin (50 μg/mL), and chloramphenicol (34 μg/mL).

Culture Medium and Cultivation Conditions. The minimal medium designed by Neidhardt et al.,[40] with 125 mM MOPS and Na_2HPO_4 in place of K_2HPO_4, supplemented with 20 g/L glycerol, 10 g/L tryptone, 5 g/L yeast extract, 100 μM $FeSO_4$, 5 mM calcium pantothenate, 1.48 mM Na_2HPO_4, 5 mM $(NH_4)_2SO_4$, and 30 mM NH_4Cl was used for all fermentations unless otherwise stated. Antibiotics (100 μg/mL ampicillin and 34 μg/mL chloramphenicol) and inducers (0.1 μM isopropyl β-D-1-thiogalactopyranoside and 100 ng/mL anhydrotetracycline) were included when appropriate. All chemicals were obtained from Fisher Scientific Co. (Pittsburgh, PA) and Sigma-Aldrich Co. (St. Louis, MO).

Fermentations were conducted in 25 mL Pyrex Erlenmeyer flasks (narrow mouth/heavy duty rim, Corning Inc., Corning, NY) filled with 20 mL of the above culture medium and sealed with foam plugs filling the necks. A single colony of the desired strain was cultivated overnight (14−16 h) in LB medium with appropriate antibiotics and used as the inoculum (1%) for all fermentations. After inoculation, flasks were incubated at 37 °C and 200 rpm in an NBS C24 Benchtop Incubator Shaker (New Brunswick Scientific Co., Inc., Edison, NJ) until an optical density of ∼0.3−0.5 was reached, at which point IPTG and anhydrotetracycline were added. Flasks were then incubated under the same conditions for 48 h post-induction unless otherwise stated.

Analytical Methods. Optical density was measured at 550 nm in a Thermo Spectronic Genesys 20 (Thermo Scientific, Waltham, MA) and used as an estimate of cell mass (1 OD_{550} = 0.34 g dry weight/L).[41] Identification of short chain ($C \leq 4$) metabolites was conducted through nuclear magnetic resonance (NMR) as previously described,[8] while longer-chain fatty acids were identified via gas chromatography−mass spectroscopy (GC−MS). Identification of fatty acids was performed on an Agilent 7890A GC system (Agilent Technologies, Santa Clara, CA), equipped with a 5975C inert XL mass selective detector (Agilent Technologies, Santa Clara, CA) and an Rxi-5Sil column (0.25 mm internal diameter, 0.10 μm film thickness, 30 m length; Restek, Bellefonte, PA), following the method of an initial temperature of 35 °C held for 1 min, 6 °C/min to 200 °C, 30 °C/min to 270 °C, held for 1 min. Extraction and derivatization procedures were as described below. Helium (2.6 mL/min, Matheson Tri-Gas, Longmont, CO) was used as the carrier gas. The injector and detector were maintained at 280 °C. A 2 μL sample was injected using a 40:1 split ratio.

Quantification of glycerol and metabolic products in the culture supernatant was conducted through high-performance liquid chromatography (HPLC) and gas chromatography-flame ionization detection (GC-FID). The concentrations of glycerol, ethanol, and organic acids were determined via ion-exclusion HPLC using a Shimadzu Prominence SIL 20 system (Shimadzu

Scientific Instruments, Inc., Columbia, MD) equipped with an HPX-87H organic acid column (Bio-Rad, Hercules, CA) with operating conditions to optimize peak separation (0.3 mL/min flow rate, 30 mM H_2SO_4 mobile phase, column temperature 42 °C).[42] Additional quantification of fatty acids (C4−C12) and fatty acid methyl esters (C14−C18) was carried out in a Varian CP-3800 gas chromatograph (Varian Associates, Inc., Palo Alto, CA), equipped with a flame ionization detector (GC-FID) and an HP-INNOWax capillary column (0.32 mm internal diameter, 0.50 μm film thickness, 30 m length; Agilent Technologies, Inc., Santa Clara, CA), following the method: 50 °C held for 3 min, 10 °C/min to 250 °C, and 250 °C held for 10 min. Helium (1.8 mL/min, Matheson Tri-Gas, Longmont, CO) was used as the carrier gas. The injector and detector were maintained at 220 and 275 °C, respectively. A 1 μL sample was injected in splitless injection mode.

For the identification of fatty acids, supernatant aliquots of 2 mL were transferred to 5 mL glass vials (Fisher Scientific Co., Pittsburgh, PA). Samples were supplemented with 1.2 μL of 1-nonanol as internal standard and extracted with 2 mL of hexane. Vials were tightly closed, vortexed for 30 s, and mixed in a Glas-Col rotator (Glas-Col, Terre Haute, IN) at 60 rpm for 2 h. Samples were then vortexed again for 30 s and centrifuged at 8000 rpm at 4 °C for 1 min. Aliquots of 700 μL of the top organic layer were transferred to 2 mL borosilicate glass vials with PTFE/silicone screw caps (Fisher Scientific Co., Pittsburgh, PA) and mixed with 50 μL of pyridine and 50 μL of BSTFA (N,O-bis(trimethylsilyl)trifluoroacetamide). Samples were incubated in sealed vials at 70 °C for 30 min using an AccuBlock Digital Dry Bath (LabNet, Woodbridge, NJ), and silylated samples were analyzed via GC−MS.

For the quantification of fatty acids and fatty acid methyl esters, supernatant aliquots of 2 mL were transferred to 5 mL glass vials (Fisher Scientific Co., Pittsburgh, PA). Samples were acidified with sulfuric acid, supplemented with 2 mg of tridecanoic acid as internal standard, and extracted with 2 mL of a mixture of hexane/chloroform (4:1, v/v). Vortex, rotation, and centrifugation were done as described above. For the quantification of short- and medium-chain fatty acids (C4−C12), 1 mL of the organic layer was aliquoted into 2 mL borosilicate glass vials with PTFE/silicone screw caps (Fisher Scientific Co., Pittsburgh, PA) and analyzed via GC-FID. For the quantification of longer-chain fatty acids (C14−C18), 1 mL of the organic layer was transferred to 2 mL glass vials (Fisher Scientific Co., Pittsburgh, PA). Samples were nitrogen evaporated to near dryness, redissolved in 1 mL of a mixture of methanol/chloroform/sulfuric acid (30:3:1, v/v/v) and incubated in a sealed vial at 90 °C for 60 min using an AccuBlock Digital Dry Bath (LabNet, Woodbridge, NJ). Water (1 mL) was added to each tube, and fatty acid methyl esters (FAMEs) were extracted with 2 mL of hexane/chloroform (4:1, v/v). After extraction, 1 mL of the organic layer was aliquoted into 2 mL borosilicate glass vials with PTFE/silicone screw caps (Fisher Scientific Co., Pittsburgh, PA) and analyzed via GC-FID.

Stearic ($C_{18:0}$), palmitic ($C_{16:0}$), myristic ($C_{14:0}$), lauric ($C_{12:0}$), capric ($C_{10:0}$), caprylic ($C_{8:0}$), caproic ($C_{6:0}$), and butyric ($C_{4:0}$) acids (Sigma Chemical Co., St. Louis, MO) were used to calibrate the gas chromatograph. Hexane (high resolution gas chromatography grade) and chloroform (reagent grade) were used as extraction solvents (Fisher Scientific Co., Pittsburgh, PA). 1-Nonanol, pyridine (HPLC grade), and BSTFA (synthesis grade) were used for the silylation reaction (Sigma Chemical Co., St. Louis, MO). Methanol and concentrated sulfuric acid used for the esterification reaction were reagent grade (Fisher Scientific Co., Pittsburgh, PA).

When stated, product yields (mmol/mmol glycerol or g/g glycerol) represent the amount of product synthesized per amount of glycerol consumed during the length of the fermentation (48 h unless otherwise stated). All values stated as different were compared with a 0.05 level of significance.

Enzymatic Characterization and Assays. For enzyme characterization, *E. coli fadA* and *fadB* genes were cloned from MG1655 genomic DNA into the pUCBB-ntH6 vector[43] to yield a constitutively expressed gene with a n-terminal His_6-tag that can be cleaved by Thrombin. *fadA* was amplified as two halves with the primers fadANdeI5p:fadAmidrev (1st half) and fadAmidfor:fadANotI3p (2nd half) (Supplementary Table S3). *fadB* was amplified in three parts with fadBNdeI5p:fadBmid1rev (1st part), fadBmid1for:fadBmid2rev (2nd part), and fadBmid2for:fadBNotI3p (3rd part) (Supplementary Table S3). *fadA* and *fadB* PCR products sections were combined by overlap extension PCR to yield the whole genes, which were subsequently digested with NdeI and NotI restriction enzymes and ligated into pUCBB-ntH6 that was previously digested with NdeI and NotI to yield pUCBB-ntH6-FadA and pUCBB-ntH6-FadB. The *hbd* gene from *Clostridium acetobutylicum* ATCC 824 (*ca*HBD) was cloned into pUCBB-pBAD[43] to yield an arabinose-inducible *ca*HBD gene with a c-terminal His_6-tag. *ca*HBD was PCR amplified from the genome of *Clostridium acetobutylicum* ATCC 824 using the caHBDBglii5p and caHBDxhoI3p primers (Supplementary Table S3). The resulting PCR product was then digested with *Bgl*II and XhoI and ligated into pUCBB-pBAD previously digested with *Bgl*II and XhoI to yield pUCBB-pBAD-caHBD. For AtoB and thioesterase characterization assays, the pCA24N- *gene* (-gfp) plasmids from the ASKA collection[44] were used. For expression of *E. gracilis* TER for kinetic characterization, the *eg*TER gene was cloned into pTrcHis2A using the In-Fusion protocol (Clontech Laboratories, Inc., Mountain View, CA) following PCR amplification from the aforementioned codon-optimized *eg*TER containing plasmid with the primer pair of F1pTH6hisEgter and R1pTH6hisEgter (Supplementary Table S3).

Cultures for enzymatic assays were grown overnight in 100 mL of LB media at 37 °C in 250 mL baffled flasks (Wheaton Industries, Inc., Millville, NJ) in *E. coli* BL21 (DE3) cells induced with either 1 mM IPTG (pCA24N, pTrcHis2A) or 1 mM Arabinose (pUCBB-pBAD) at an OD_{600} of ∼0.6 or expressed constitutively (pUCBB-ntH6). Reactions were monitored on either a Synergy HT plate reader (BioTek Instruments, Inc., Winooski, VT) at 25 °C (for reactions monitored at 300 nm or higher) or in a Biomate 5 Spectrophotometer (Thermo Scientific, Waltham, MA) for reactions at 263 nm. Cells were lysed using Bacterial Protein Extraction Reagent (B-PER) (Thermo Scientific, Waltham, MA) as per the prescribed protocol in order to obtain the supernatant containing the active enzymes. FadE and YdiO were purified following previously established methods[45] using the same growth conditions mentioned above. Cell pellets were resuspended in 40 mL of 50 mM potassium phosphate buffer pH 7.2 and broken by disruption EmulsiFlex-C5 homogenizer (Avestin, Ottawa, ON). Disrupted cells were then spun for 90 min at 4 °C at 120,000*g* in a Optima L-80XP Ultracentrifuge (Beckman-Coulter, Schaumburg, IL) to produce the supernatant used for assays. For specific activity assays (reported in μmol substrate/mg protein/min) these supernatant fractions

dx.doi.org/10.1021/sb3000782 | *ACS Synth. Biol.* 2012, 1, 541−554

were utilized and protein concentration was established using the Bradford Reagent (Thermo Scientific, Waltham, MA) using BSA as the protein standard. Linearity was established for each reaction and the background nonenzymatic rate was subtracted to establish the activity.

For kinetic characterization, his-tagged proteins of AtoB, FadA, FadB, *ca*HBD, *eg*TER were purified from the B-PER supernatant fractions using Talon Metal Affinity Resin (Clontech Laboratories, Inc., Mountain View, CA) using gravity purification. In short, the supernatant was mixed for 1 h at room temperature on a LabQuake rotator (Fisher Scientific, Pittsburgh, PA) with approximately 2 mL of Talon Resin (1 mL resin/0.3 mg supernatant protein) that was prewashed twice with Buffer A (50 mM Tris pH 7.9, 5 mM $MgCl_2$, 100 mM NaCl, 5 mM imidazole). Resin was then spun at 700*g* for 5 min to remove the nonbound proteins, washed with 20x (40 mL) Buffer A, resuspended in 20x (40 mL) Buffer B (Buffer A with 20 mM Imidazole), and loaded onto a gravity column. Buffer B was then drained off, and the protein was eluted with 20 mL of Buffer C (Buffer A with 250 mM imidazole). The eluted fraction was then concentrated and used for kinetic characterizations. Enzyme concentration was established by measuring the absorbance at 260 nm, and extinction coefficients were predicted for each enzyme by the ProtParam program (http://web.expasy.org/protparam/).

For kinetic characterization, an appropriate amount of enzyme was established by checking linear range near predicted K_M values. Then, the rates were measured for a range of substrates in order to establish k_{cat} and K_M. In the cases of FadB for the crotonase reaction and FadA in the "forward" thiolase reaction coupled with HBD, substrate saturation could not be established, and as such, the k_{cat}/K_M for the reaction was determined by dividing the linear slope of Velocity vs [Substrate] by the amount of enzyme used in the assays. For reactions that could be saturated, Velocity vs [Substrate] was fitted by the EnzKIN Matlab module (http://www.mathworks.com/matlabcentral/fileexchange/26653) to establish V_{max} and K_M. All values stated as different were compared with a 0.05 level of significance.

The forward thiolase assay (i.e., biosynthetic direction) and β-hydroxybutyryl-CoA dehydrogenase assays were performed in the presence of 1.5 mM DTT, 4.5 mM $MgCl_2$, 100 mM Tris HCl pH 7.5, and 0.2 mM NADH in a total volume of 200 μL at 25 °C.[46] β-Hydroxybutyryl-CoA dehydrogenase activity was monitored by following the oxidation of NADH at 340 nm, while thiolase activity in the forward direction was measured at 340 nm in a coupled assay in which 10 U excess of *ca*HBD was present to reduce the acetoacetyl-CoA generated from thiolase activity. Thiolase activity in the reverse direction was determined in the presence of 0.5 mM DTT, 4.5 mM $MgCl_2$, 100 mM Tris HCl pH 7.5, and 2 mM CoA in a total volume of 200 μL at 25 °C.[47] Activity was monitored by the loss of acetoacetyl-CoA at 303 nm using an extinction coefficient of 14 mM^{-1} cm^{-1}. Crotonase activity was monitored by following the loss of crotonoyl-CoA at 263 nm (ε = 6.7 mM^{-1} cm^{-1}) in the presence of 100 mM Tris HCL pH 7.5 in 200 μL total volume.[48] For *eg*TER, crotonyl-CoA reductase activity was followed by monitoring the loss of NADH absorbance in the presence of 100 mM Tris HCL pH 7.5 and 0.2 mM NADH in a final volume of 200 μL at 25 °C.[46] For FadE and YdiO, Butyryl-CoA dehydrogenase activity was measured utilizing ferricenium ion.[49] Reactions were performed in 50 mM potassium phosphate pH 7.2, 0.4 mM $MgSO_4$, 200 μM ferrocenium hexafluorophosphate, and 200 μM Butyryl-CoA and the formation of the reduced ferrocene ion was monitored at 300 nm (ε = 4.3 mM^{-1} cm^{-1}). Thioesterase activity was monitored by following the production of TNB at 412 nm (ε = 4.3 mM^{-1} cm^{-1}).[30] Reactions were carried out in the presence of 100 mM Tris pH 7.5, 200 mM KCl, 25 mM DTNB and 200 μM of the "-CoA" substrate in a volume of 200 μL at 25 °C. All substrates and chemicals for enzyme assays were obtained from Fisher Scientific Co. (Pittsburgh, PA) and Sigma-Aldrich Co. (St. Louis, MO).

■ ASSOCIATED CONTENT

Supporting Information

Supporting tables with full details of strains, plasmids, and primers used in this study. This material is available free of charge via the Internet at http://pubs.acs.org.

■ AUTHOR INFORMATION

Corresponding Author

*Tel: (713) 348-4893. Fax: (713) 348-5478. E-mail: Ramon.Gonzalez@rice.edu.

Author Contributions

J.M.C., J.E.V., and R.G. designed the experiments. J.M.C. constructed the strains and conducted all strain characterization experiments. J.E.V. preformed all enzymatic characterization experiments. M.D.B. constructed the plasmids. M.R.M. preformed the GC and GC−MS analysis. J.M.C. and R.G. drafted the manuscript. All authors read, edited, and approved the final manuscript.

Notes

The authors declare no competing financial interest.

■ ACKNOWLEDGMENTS

The authors wish to thank E. N. Miller for assistance with plasmid construction; Q. Kleerekoper for assistance with NMR techniques; and D. Castillo-Rivera, B. Wilson, and S.P.T. Matsuda for assistance with GC−MS techniques. This work was supported by grants from the U.S. National Science Foundation (EEC-0813570, CBET-1134541, CBET-1067565).

■ REFERENCES

(1) Rude, M. A., and Schirmer, A. (2009) New microbial fuels: a biotech perspective. *Curr. Opin. Microbiol. 12*, 274−281.

(2) Connor, M. R., and Liao, J. C. (2009) Microbial production of advanced transportation fuels in non-natural hosts. *Curr. Opin. Biotechnol. 20*, 307−315.

(3) Lee, J. W., Na, D., Park, J. M., Lee, J., Choi, S., and Lee, S. Y. (2012) Systems metabolic engineering of microorganisms for natural and non-natural chemicals. *Nat. Chem. Biol. 8*, 536−546.

(4) Peralta-Yahya, P. P., Zhang, F., del Cardayre, S. B., and Keasling, J. D. (2012) Microbial engineering for the production of advanced biofuels. *Nature 488*, 320−328.

(5) Steen, E. J., Kang, Y. S., Bokinsky, G., Hu, Z. H., Schirmer, A., McClure, A., del Cardayre, S. B., and Keasling, J. D. (2010) Microbial production of fatty-acid-derived fuels and chemicals from plant biomass. *Nature 463*, 559−U182.

(6) Handke, P., Lynch, S. A., and Gill, R. T. (2011) Application and engineering of fatty acid biosynthesis in *Escherichia coli* for advanced fuels and chemicals. *Metab. Eng. 13*, 28−37.

(7) Lennen, R. M., Braden, D. J., West, R. M., Dumesic, J. A., and Pfleger, B. F. (2010) A process for microbial hydrocarbon synthesis: Overproduction of fatty acids in *Escherichia coli* and catalytic conversion to alkanes. *Biotechnol. Bioeng. 106*, 193−202.

(8) Dellomonaco, C., Clomburg, J. M., Miller, E. N., and Gonzalez, R. (2011) Engineered reversal of the β-oxidation cycle for the synthesis of fuels and chemicals. *Nature 476*, 355−359.
(9) Keasling, J. D. (2008) Synthetic biology for synthetic chemistry. *ACS Chem. Biol. 3*, 64−76.
(10) Clomburg, J. M., and Gonzalez, R. (2010) Biofuel production in *Escherichia coli*: the role of metabolic engineering and synthetic biology. *Appl. Microbiol. Biotechnol. 86*, 419−434.
(11) Clark, D. P., and Cronan, J. E. (2005) Two-carbon compounds and fatty acids as carbon sources, in *EcoSal-Escherichia coli and Salmonella: cellular and molecular biology* (Neidhardt, F., Curtiss, R. I., Ingraha, J., Lin, E., Low, K., Magasanik, B., Reznikoff, W., Riley, N., Schaechter, M., and Umbarger, H., Eds.) 2nd ed., ASM Press, Washington, DC.
(12) Feigenbaum, J., and Schulz, H. (1975) Thiolases of *Escherichia coli*: purification and chain-length specificities. *J. Bacteriol. 122*, 407−411.
(13) Jenkins, L. S., and Nunn, W. D. (1987) Genetic and molecular characterization of the genes involved in short-chain fatty-acid degradation in *Escherichia coli:* The Ato system. *J. Bacteriol. 169*, 42−52.
(14) Yang, S. Y., Yang, X. Y. H., Healy-Louie, G., Schulz, H., and Elzinga, M. (1990) Nucleotide sequence of the *fadA* gene: Primary structure of the 3-ketoacyl-coenzyme A thiolase from *Escherichia coli* and the structural organization of the *fadBA* operon. *J. Biol. Chem. 265*, 10424−10429.
(15) Nielsen, J., Villadsen, J., and Liden, G. (2003) *Bioreaction Engineering Principles*, Kluwer Adademic/Plenum Publishers, New York.
(16) Teufel, R., Mascaraque, V., Ismail, W., Voss, M., Perera, J., Eisenreich, W., Haehnel, W., and Fuchs, G. (2010) Bacterial phenylalanine and phenylacetate catabolic pathway revealed. *Proc. Natl. Acad. Sci. U.S.A. 107*, 14390−14395.
(17) Binstock, J. F., and Schulz, H. (1981) Fatty acid oxidation complex from *Escherichia coli*. *Methods Enzymol. 71*, 403−411.
(18) He, X. Y., and Yang, S. Y. (1997) Glutamate-119 of the large alpha-subunit is the catalytic base in the hydration of 2-trans-enoyl-coenzyme A catalyzed by the multienzyme complex of fatty acid oxidation from *Escherichia coli*. *Biochemistry 36*, 11044−11049.
(19) Campbell, J. W., Morgan-Kiss, R. M., and Cronan, J. E. (2003) A new *Escherichia coli* metabolic competency: growth on fatty acids by a novel anaerobic β-oxidation pathway. *Mol. Microbiol. 47*, 793−805.
(20) Gulevich, A. Y., Skorokhodova, A. Y., Sukhozhenko, A. V., Shakulov, R. S., and Debabov, V. G. (2012) Metabolic engineering of *Escherichia coli* for 1-butanol biosynthesis through the inverted aerobic fatty acid β-oxidation pathway. *Biotechnol. Lett. 34*, 463−469.
(21) Eichler, K., Bourgis, F., Buchet, A., Kleber, H. P., and Mandrandberthelot, M. A. (1994) Molecular characterization of the *Cai* operon necessary for carnitine metabolism in *Escherichia coli*. *Mol. Microbiol. 13*, 775−786.
(22) Walt, A., and Kahn, M. L. (2002) The *fixA* and *fixB* genes are necessary for anaerobic carnitine reduction in *Escherichia coli*. *J. Bacteriol. 184*, 4044−4047.
(23) Eichler, K., Buchet, A., Bourgis, F., Kleber, H. P., and Mandrandberthelot, M. A. (1995) The *fix Escherichia coli* region contains 4 genes related to carnitinie metabolism. *J. Basic Microbiol. 35*, 217−227.
(24) Akhtar, M. K., and Jones, P. R. (2009) Construction of a synthetic YdbK-dependent pyruvate:H-2 pathway in *Escherichia coli* BL21(DE3). *Metab. Eng. 11*, 139−147.
(25) Hoffmeister, M., Piotrowski, M., Nowitzki, U., and Martin, W. (2005) Mitochondrial trans-2-enoyl-CoA reductase of wax ester fermentation from *Euglena gracilis* defines a new family of enzymes involved in lipid synthesis. *J. Biol. Chem. 280*, 4329−4338.
(26) Inui, H., Miyatake, K., Nakano, Y., and Kitaoka, S. (1984) Fatty acid synthesis in mitochondria of *Euglena gracilis*. *Eur. J. Biochem. 142*, 121−126.
(27) Inui, H., Miyatake, K., Nakano, Y., and Kitaoka, S. (1983) Production and composition of wax esters by fermentation of *Euglena gracilis*, *Agric. Biol. Chem. 47*, 2669−2671.
(28) Cho, H. S., and Cronan, J. E. (1993) *Escherichia coli* thioesterase I, molecular cloning and sequencing of the structural gene and identification as a periplasmic enzyme. *J. Biol. Chem. 268*, 9238−9245.
(29) Nie, L., Ren, Y., Janakiraman, A., Smith, S., and Schulz, H. (2008) A novel paradigm of fatty acid β-oxidation exemplified by the thioesterase-dependent partial degradation of conjugated linoleic acid that fully supports growth of *Escherichia coli*. *Biochemistry 47*, 9618−9626.
(30) Zhuang, Z. H., Song, F., Zhao, H., Li, L., Cao, J., Eisenstein, E., Herzberg, O., and Dunaway-Mariano, D. (2008) Divergence of function in the hot dog fold enzyme superfamily: The bacterial thioesterase YciA. *Biochemistry 47*, 2789−2796.
(31) Feng, Y., and Cronan, J. E. (2009) A new member of the *Escherichia coli fad* regulon: Transcriptional regulation of *fadM* (*ybaW*). *J. Bacteriol. 191*, 6320−6328.
(32) Kuznetsova, E., Proudfoot, M., Sanders, S. A., Reinking, J., Savchenko, A., Arrowsmith, C. H., Edwards, A. M., and Yakunin, A. F. (2005) Enzyme genomics: Application of general enzymatic screens to discover new enzymes. *FEMS Microbiol. Rev. 29*, 263−279.
(33) Vlessis, A. A., Bartos, D., and Trunkey, D. (1990) Importance of spontaneous alpha-ketoacid decarboxylation in experiments involving peroxide. *Biochem. Biophys. Res. Commun. 170*, 1281−1287.
(34) Yazdani, S. S., and Gonzalez, R. (2007) Anaerobic fermentation of glycerol: a path to economic viability for the biofuels industry. *Curr. Opin. Biotechnol. 18*, 213−219.
(35) Kang, Y. S., Durfee, T., Glasner, J. D., Qiu, Y., Frisch, D., Winterberg, K. M., and Blattner, F. R. (2004) Systematic mutagenesis of the *Escherichia coli* genome. *J. Bacteriol. 186*, 8548−8548.
(36) Yazdani, S. S., and Gonzalez, R. (2008) Engineering *Escherichia coli* for the efficient conversion of glycerol to ethanol and co-products. *Metab. Eng. 10*, 340−351.
(37) Miller, J. H. (1972) *Experiments in Molecular Genetics*, Cold Spring Harbor Laboratory Press, Cold Spring Harbor, NY.
(38) Baba, T., Ara, T., Hasegawa, M., Takai, Y., Okumura, Y., Baba, M., Datsenko, K. A., Tomita, M., Wanner, B. L., and Mori, H. (2006) Construction of *Escherichia coli* K-12 in-frame, single-gene knockout mutants: the Keio collection. *Mol. Syst. Biol. 2*, 11.
(39) Sambrook, J., Fritsch, E. F., Maniatis, T., Russell, D. W. (2001) *Molecular Cloning: A Laboratory Manual*, 3rd ed., Cold Spring Harbor Laboratory Press, Cold Spring Harbor, NY.
(40) Neidhardt, F. C., Bloch, P. L., and Smith, D. F. (1974) Culture medium for enterobacteria. *J. Bacteriol. 119*, 736−747.
(41) Dharmadi, Y., Murarka, A., and Gonzalez, R. (2006) Anaerobic fermentation of glycerol by *Escherichia coli*: A new platform for metabolic engineering. *Biotechnol. Bioeng. 94*, 821−829.
(42) Dharmadi, Y., and Gonzalez, R. (2005) A better global resolution function and a novel iterative stochastic search method for optimization of high-performance liquid chromatographic separation. *J Chromatogr., A 1070*, 89−101.
(43) Vick, J. E., Johnson, E. T., Choudhary, S., Bloch, S. E., Lopez-Gallego, F., Srivastava, P., Tikh, I. B., Wawrzyn, G. T., and Schmidt-Dannert, C. (2011) Optimized compatible set of BioBrick (TM) vectors for metabolic pathway engineering. *Appl. Microbiol. Biotechnol. 92*, 1275−1286.
(44) Kitagawa, M., Ara, T., Arifuzzaman, M., Ioka-Nakamichi, T., Inamoto, E., Toyonaga, H., and Mori, H. (2005) Complete set of ORF clones of *Escherichia coli* ASKA library (A complete Set of *E. coli* K-12 ORF archive): Unique resources for biological research. *DNA Res. 12*, 291−299.
(45) Obrien, W. J., and Frerman, F. E. (1977) Evidence for a complex of 3 β-oxidation enzymes in *Escherichia coli*: Induction and localization. *J. Bacteriol. 132*, 532−540.
(46) Bond-Watts, B. B., Bellerose, R. J., and Chang, M. C. Y. (2011) Enzyme mechanism as a kinetic control element for designing synthetic biofuel pathways. *Nat. Chem. Biol. 7*, 222−227.

(47) Wiesenborn, D. P., Rudolph, F. B., and Papoutsakis, E. T. (1988) Thiolase from *Clostridium acetobutylicum* ATCC-824 and its role in the synthesis of acids and solvents. *Appl. Environ. Microbiol. 54*, 2717−2722.
(48) Hartmanis, M. G. N., and Gatenbeck, S. (1984) Intermediary metabolism in *Clostridium acetobutylicum*: Levels of enzymes involved in the formation of acetate and butyrate. *Appl. Environ. Microbiol. 47*, 1277−1283.
(49) Lehman, T. C., Hale, D. E., Bhala, A., and Thorpe, C. (1990) An acyl-coenzyme A dehydrogenase assay utilizing the feericenium ion. *Anal. Biochem. 186*, 280−284.